

GEOCARBSULF: A combined model for Phanerozoic atmospheric O₂ and CO₂

Robert A. Berner *

Department of Geology and Geophysics, Yale University, New Haven, CT 06520-8109, USA

Received 13 June 2005; accepted in revised form 1 November 2005

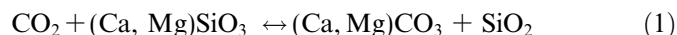
Abstract

A model for the combined long-term cycles of carbon and sulfur has been constructed which combines all the factors modifying weathering and degassing of the GEOCARB III model [Berner R.A., Kothavala Z., 2001. GEOCARB III: a revised model of atmospheric CO₂ over Phanerozoic time. *Am. J. Sci.* **301**, 182–204] for CO₂ with rapid recycling and oxygen dependent carbon and sulfur isotope fractionation of an isotope mass balance model for O₂ [Berner R.A., 2001. Modeling atmospheric O₂ over Phanerozoic time. *Geochim. Cosmochim. Acta* **65**, 685–694]. New isotopic data for both carbon and sulfur are used and new feedbacks are created by combining the models. Sensitivity analysis is done by determining (1) the effect on weathering rates of using rapid recycling (rapid recycling treats carbon and sulfur weathering in terms of young rapidly weathering rocks and older more slowly weathering rocks); (2) the effect on O₂ of using different initial starting conditions; (3) the effect on O₂ of using different data for carbon isotope fractionation during photosynthesis and alternative values of oceanic δ¹³C for the past 200 million years; (4) the effect on sulfur isotope fractionation and on O₂ of varying the size of O₂ feedback during sedimentary pyrite formation; (5) the effect on O₂ of varying the dependence of organic matter and pyrite weathering on tectonic uplift plus erosion, and the degree of exposure of coastal lands by sea level change; (6) the effect on CO₂ of adding the variability of volcanic rock weathering over time [Berner, R.A., 2006. Inclusion of the weathering of volcanic rocks in the GEOCARBSULF model. *Am. J. Sci.* **306** (in press)]. Results show a similar trend of atmospheric CO₂ over the Phanerozoic to the results of GEOCARB III, but with some differences during the early Paleozoic and, for variable volcanic rock weathering, lower CO₂ values during the Mesozoic. Atmospheric oxygen shows a major broad late Paleozoic peak with a maximum value of about 30% O₂ in the Permian, a secondary less-broad peak centered near the Silurian/Devonian boundary, variation between 15% and 20% O₂ during the Cambrian and Ordovician, a very sharp drop from 30% to 15% O₂ at the Permo-Triassic boundary, and a more-or less continuous rise in O₂ from the late Triassic to the present.

© 2006 Elsevier Inc. All rights reserved.

1. Introduction

The controls of levels of atmospheric O₂ and CO₂ on a multimillion year time scale can be summarized by just three very succinct chemical reactions first written or described in words by Ebelmen (1845) and independently deduced much later by Urey (1952); Holland (1978) and Garrels and Perry (1974). (For further details on these reactions consult Berner, 2004). They are;



Reaction (1), going from left-to-right represents the summation of weathering of calcium and magnesium silicate minerals by CO₂ (derived ultimately from the atmosphere), with the formation of Ca²⁺ and Mg²⁺, HCO₃⁻ and H₄SiO₄ in solution, followed by the transport of these solutes to the sea where they are deposited as Ca and Mg carbonates and biogenic silica. Reaction (1) written from right-to-left represents the thermal decomposition of carbonates via volcanism, metamorphism and diagenesis with the release of

* Fax: +1 203 432 3134.

E-mail address: robert.berner@yale.edu

CO₂ to the atmosphere and oceans along with the formation of Ca and Mg silicates. This reaction exerts the major control on atmospheric CO₂.

Both CO₂ and O₂ are affected by reaction (2). Going from left-to-right this reaction represents the burial in sediments of organic matter formed ultimately by photosynthesis. Going from right-to-left the reaction represents either the oxidative weathering on the continents of old sedimentary organic matter or the thermal decomposition at depth of the organic matter with the resulting reduced carbon gases emitted to and oxidized in the atmosphere and oceans. This reaction exerts the major control on atmospheric O₂.

Reaction (3) reading from left-to-right represents the oxidative weathering of pyrite on the continents or the thermal decomposition of pyrite at depth with the resulting reduced sulfur gases emitted to and oxidized in the atmosphere and oceans. Reading from right-to-left the reaction represents the summation of photosynthesis, bacterial sulfate reduction and sedimentary pyrite formation. Reaction (3) expresses the effects of the global sulfur cycle on atmospheric O₂.

Computer modeling of the combined carbon and sulfur cycles in order to calculate levels of O₂ and CO₂ over millions of years has been done by Francois and Walker (1992); Godderis et al. (2001); Hansen and Wallmann (2003); Bergman et al. (2004) and Arvidson and Mackenzie (2006). Earlier work by the writer was on modeling separately the evolution of CO₂ in terms of the GEOCARB model (Berner and Kothavala, 2001) and an isotopic mass balance model for O₂ (Berner, 1987, 2001). The

GEOCARB III model has recently been amended (Berner, *in press*) to include the effects on CO₂ of changing volcanic weathering over time. The purpose of the present paper is to combine the isotope mass balance and GEOCARB models to produce a combined model, here labeled as GEOCARBSULF, that enables calculation of both CO₂ and O₂. In doing this, such concepts as rapid recycling (Berner, 1987; Berner and Canfield, 1989) and O₂-dependence of carbon and sulfur isotope fractionation (Berner, 2001) are introduced to GEOCARB modeling. In turn the application of non-dimensional factors affecting weathering (e.g., mountain uplift and erosion) that have been applied to the GEOCARB model, are added to the isotope mass balance modeling for sulfur. To update the model new data for the carbon and sulfur isotopic composition of the oceans, as represented by measurements on carbonate and sulfate minerals, are used. These data, are summarized in Fig. 1.

2. GEOCARBSULF modeling

2.1. Fundamentals

Details of the GEOCARB and isotope mass balance modeling, combined here to form the GEOCARBSULF model, can be found in earlier papers by the author or in Berner (2004). Discussion in this paper is confined mostly to new effects that arise from combining the earlier models. However, some fundamentals of the earlier models bear repetition. In the earlier GEOCARB and isotope mass balance models, and that of the present one, calculation is done in terms of a succession of steady states for exchanges of total carbon and total sulfur between rocks and the surficial system (ocean + atmosphere + life + soils) calculated for each one million year time step. This approach is justified for carbon because of the rapidity of the re-attainment of steady state after perturbation (Sundquist, 1991). The residence time of carbon in seawater (the largest surficial reservoir) is only about 0.1 million years. However, because of the longer residence time of sulfate in seawater (about 14 million years) the assumption of steady state for sulfur is less justified.

In GEOCARB and the present GEOCARBSULF modeling the level of atmospheric CO₂ is calculated from an expression for the flux of HCO₃⁻ from Ca and Mg silicate weathering. This flux is a function of many time-dependent non-dimensional (normalized to the present) weathering parameters which are together multiplied times the present Ca–Mg silicate weathering rate. These parameters represent erosion, river runoff, plant evolution, volcanic weathering, global CO₂ degassing and land area. In addition to these parameters, the weathering expression for the silicates contains an additional non-dimensional term that includes, among other things, the feedback effects of CO₂ on temperature and plant growth as they affect CO₂ uptake via weathering. Determination at each time step of the non-dimensional variables and the actual weathering flux

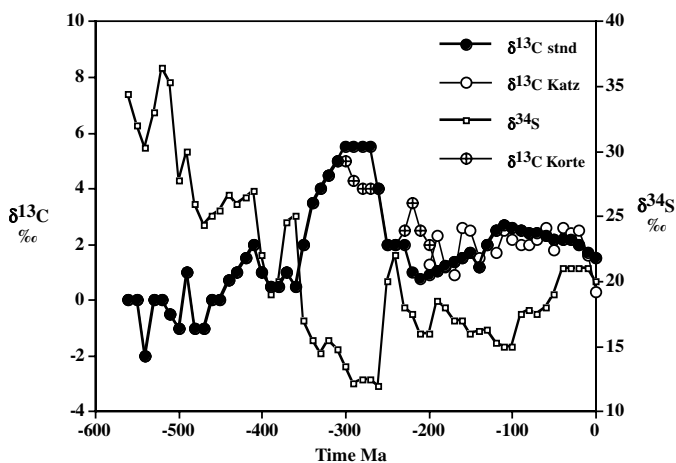


Fig. 1. Isotopic data for carbonate-C and sulfate-S used in GEOCARBSULF modeling. Stnd stands for standard formulation. $\delta^{34}\text{S}$ data from Kampschulte and Strauss (2004); $\delta^{13}\text{C}$ data from: Cambrian (550–490 Ma) Kirschvink and Raub (2003); Ordovician to Devonian (490–360 Ma) Saltzman (2005) and Veizer et al. (1999); Carboniferous to Late Permian (360–270 Ma) Popp et al. (1986), Veizer et al. (1999), and Mii et al. (1997, 2001). Alternate for Permian (300–270 Ma) Korte et al. (2005a). Late Permian to Mid-Triassic (270–240 Ma) compiled by Berner (2005). Mid to Late Triassic (240–200 Ma) Lindh (1983). Alternate Korte et al. (2005b) Jurassic to present (200–0 Ma) Lindh (1983). Alternate Katz et al. (2005).

(calculated from carbon and carbon isotope mass balance) enables calculation of the value of the temperature-CO₂ feedback term and from this the value of RCO₂ by inversion. The parameter RCO₂ is the ratio of the mass of atmospheric CO₂ at some past time to that for the pre-industrial present. The application of non-dimensional parameters affecting weathering are applied in the present paper to the weathering rates for organic carbon, pyrite sulfur, and CaSO₄ sulfur which was not done in the Berner (2001) isotope mass balance model. The appropriate equations for these are presented in the section below on land area, relief and erosion.

The level of atmospheric O₂ is calculated simply by the difference in O₂ input from organic carbon and pyrite sulfur burial and O₂ removal by weathering of organic C and pyrite S in rocks plus the oxidation of reduced C and S containing gases emitted by volcanism and metamorphism. Burial rates of organic C and pyrite S are calculated from weathering and metamorphic/volcanic fluxes via isotope mass balance equations (Berner, 2001, 2004). Rates of degassing by volcanism and metamorphism are guided by changes in sea floor spreading rate. The time step is one million years and the calculation is started at 570 Ma and run forward to the present. (For “spin-up” purposes appropriate input parameters from 570 to 550 Ma were assumed to have the same values as known values for the beginning of the Cambrian at 545 Ma.) Inverse modeling starting at present and running backward in time (K. Fennel personal communication) results in answers similar to those found for O₂ by forward modeling.

2.2. Rapid recycling and O₂

Rapid recycling (Garrels and Mackenzie, 1971; Berner, 1987), which provides negative feedback against excessive O₂ variation (Berner and Canfield, 1989; Berner, 2001), was applied to the GEOCARBSULF modeling. With rapid recycling it is assumed that the carbon and sulfur compounds in younger rocks weather faster than in older rocks which is a geologically reasonable assumption because the younger rocks are better exposed to erosion at the earth surface. Negative feedback is provided by the exposure of organic matter and pyrite rich rocks to O₂ uptake via weathering “shortly” (on a multimillion year time scale) after the deposition of the same rocks that resulted originally in excessive O₂ production. This may occur as a result of sea level drop or tectonic uplift. (Minor negative feedback also for CO₂ is provided by the exposure to weathering of limestones “shortly” after deposition.)

The actual starting values for the relative sizes, isotopic composition, and rates of weathering of organic-C, carbonate-C, CaSO₄-S and pyrite-S in “young” and “old” rocks were adjusted to give both appreciable negative feedback, geologically reasonable mean ages for the young rocks over time, and final values for O₂ equal to that at present. The mean age for a young rock is calculated as the ratio of its mass to the aging rate or rate of conversion to old rocks,

in essence a mean residence time. The aging rate is assumed to be equal to the weathering rate of carbon and sulfur compounds in the old rocks plus their thermal destruction by metamorphism and volcanism. In this way the masses of each form of carbon and sulfur in the old rocks remain constant. Allowing the old rocks to vary in mass was found to have negligible effect because of their very long residence times (400–600 million years) relative to the time span of the Phanerozoic (550 million years). Additional contribution to volcanic and metamorphic degassing by the subduction of seafloor, which by definition has not undergone continental weathering, is added to the degassing flux for the old rocks. (Submarine weathering of basalt is considered minor compared to continental weathering—see Berner, 2004).

Plots of mean age for young organic matter, carbonates, pyrite, and calcium sulfate are shown in Figs. 2 and 3. The large variation and lower values for mean age of young organic carbon, compared to that for young carbonate carbon is due mainly to changes in the young organic abundance. At any time there was a much lower mass of young organic matter globally than that for carbonate, lower masses lead to shorter mean ages (in other words, shorter residence times) and greater variability. Fig. 3 shows that mean ages of CaSO₄ were lower than for pyrite, in this case the lower mean age is due mainly to more rapid turnover, not just lower masses of CaSO₄ sulfur compared to pyrite sulfur. This is keeping with the idea that CaSO₄ weathers faster than pyrite (see discussion below). The very high mean ages of young pyrite during the early Paleozoic are due to the accumulation of large masses of pyrite at that time due to the presence of an ocean with anoxic bottom waters (Berner and Raiswell, 1983; Wilde, 1987).

Plots of the relative rates of weathering of young vs old organic matter, carbonates, pyrite, and calcium sulfate are shown in Figs. 4 and 5. Note that the ratios of weathering

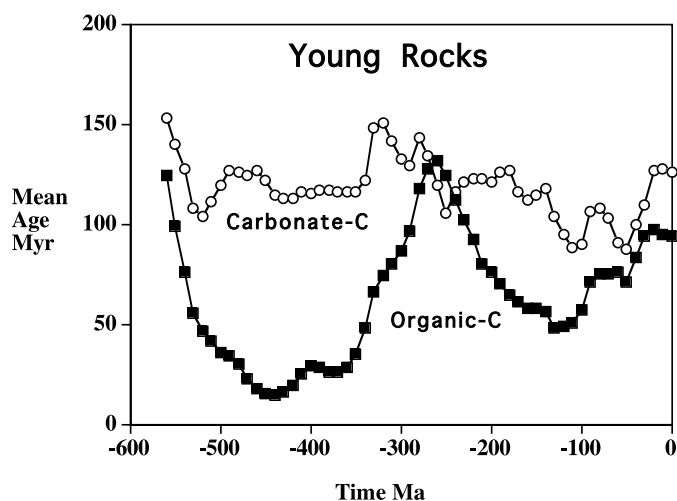


Fig. 2. Mean age of young carbonate carbon and organic carbon as a function of time. Mean age is defined as young mass/young-to-old aging flux (see text under rapid recycling).

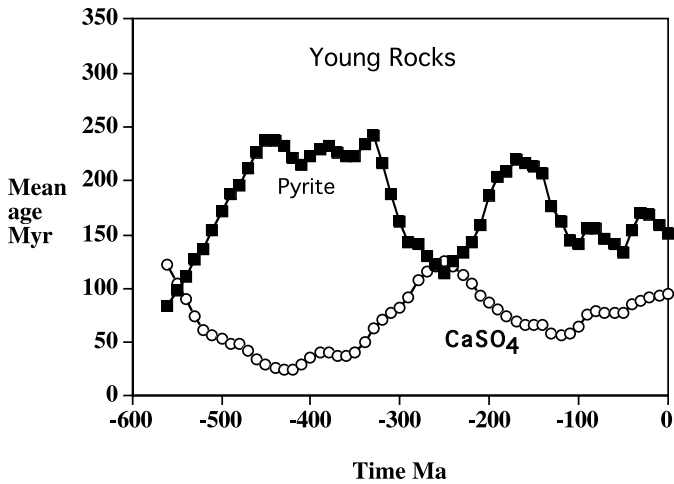


Fig. 3. Mean age of young pyrite and CaSO_4 as a function of time. (For definition see caption to Fig. 2).

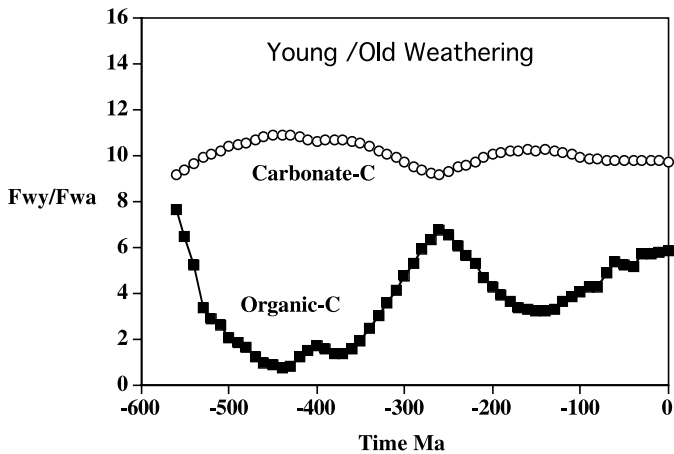


Fig. 4. Ratio of rates of weathering of young/old (F_{wy}/F_{wa}) carbonate and organic matter as a function of time.

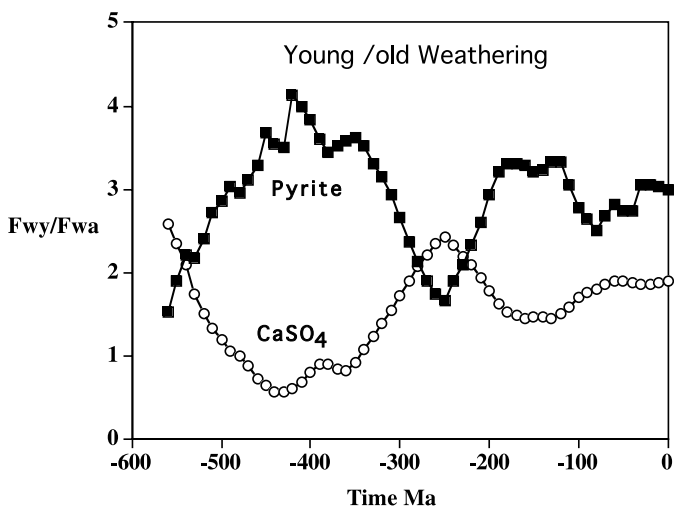


Fig. 5. Ratio of rates of weathering of young/old (F_{wy}/F_{wa}) pyrite and CaSO_4 as a function of time.

rates for organic carbon vary considerably with time. This is because the amount of young organic carbon varies so much that at times, such as the early Paleozoic, very low masses of young material result in weathering rates that are about the same as those for the much more abundant old organic carbon (weathering rate ratio, $F_{wy}/F_{wa} \approx 1$). (In all isotope mass balance modeling—e.g., Garrels and Lerman, 1984—weathering rate is assumed to be directly proportional to the mass of the material undergoing weathering.) In the case of CaSO_4 (Fig. 5), reduction of young masses to such low values during the early Paleozoic results in the rate of weathering of old CaSO_4 being faster than that for young CaSO_4 ($F_{wy}/F_{wa} < 1$). At the same time the ratio of young/old pyrite weathering reaches a maximum for the whole Phanerozoic because of the deposition of such large amounts of young pyrite due to an early Paleozoic ocean with extensive anoxic bottom waters, (Berner and Raiswell, 1983; Wilde, 1987). Finally, one can see from Figs. 4 and 5 that the weathering rate ratio for CaCO_3 is much higher than that for CaSO_4 . This reflects the idea that CaSO_4 occurs in beds that are so extremely soluble that old rocks can rapidly dissolve in the subsurface leading to lesser differences in the weathering of young and old CaSO_4 . By contrast the range of weathering rate ratios for organic matter and for pyrite are similar reflecting the fact that both occur as minor components disseminated in shales, and weathering of them requires exposure to O_2 by continued loss by weathering and erosion of the enclosing rock.

2.3. Initial values and O_2

In doing the GEOCARBSULF modeling, it was found that there was sensitivity of results for O_2 over time to the assumed starting conditions at 570 Ma. This is to be expected. Once proper starting conditions were adopted so as to end at correct present day values, resulting plots of O_2 vs time were found to closely parallel those for $\delta^{13}\text{C}$ (compare Fig. 1 with Fig. 20) showing that external forcing and not initial conditions was the major control of results.

An important cause of sensitivity to starting conditions was the division into young, rapidly weathering and old, slower weathering rocks containing carbon and sulfur (rapid recycling). Initial values were adjusted so that geologically reasonable initial values still allowed the attainment at the end of the run at $t = 0$ of values of O_2 , CO_2 , organic matter burial, the sulfur/organic carbon ratio of sediments, and the isotopic composition of carbonates close to measured ones. The adopted initial (standard) values are shown in Table 1.

The effects of variation of starting values around the standard values of Table 1 were examined. Variation of the initial masses of atmospheric O_2 ($\pm 50\%$) and the initial isotopic compositions of young carbonates ($\pm 2\%$), young and old organic matter ($\pm 10\%$), young sulfates ($\pm 10\%$) and young and old pyrite ($\pm 10\%$) resulted in negligible

Table 1

Initial values at 550 Ma for GEOCARBSULF modeling

Mass of atmospheric oxygen = 25 (present = 38)
 Gy (mass of young organic carbon) = 1000
 Ga (mass of old organic carbon) = 4000
 Cy (mass of young carbonate carbon) = 250
 Ca (mass of old carbonate carbon) = 1000
 Spy (mass of young pyrite sulfur) = 20
 Spa (mass of old pyrite sulfur) = 280
 Ssy (mass of young CaSO₄ sulfur) = 150
 Ssa (mass of old CaSO₄ sulfur) = 150
 kwpy (rate constant for young pyrite weathering) = 0.01 my⁻¹
 kwpy (rate constant for young CaSO₄ weathering) = 0.01 my⁻¹
 kwpy (rate constant for young organic matter weathering) = 0.018 my⁻¹
 kwpy (rate constant for young carbonate weathering) = 0.018 my⁻¹
 δgy (δ¹³C of young organic carbon) = -23.5‰
 δga (δ¹³C of old organic carbon) = -23.5‰
 δpy (δ³⁴S of young pyrite sulfur) = -10‰
 δpa (δ³⁴S of old pyrite sulfur) = -10‰
 δcy (δ¹³C of young carbonate carbon) = 3‰
 δsy (δ³⁴S of young CaSO₄ sulfur) = 35‰

All masses in 10¹⁸ moles.

change in calculated values of O₂ over time. (Initial values of δ¹³C for old carbonate C and δ³⁴S for old sulfate S are constrained by these values, by the mean values for δ¹³C and δ³⁴S of the crust, and by the masses of young and old rocks shown in Table 1). Variation from 50% to 200% of the values shown in Table 1 for the initial mass of young pyrite sulfur (Spy) and the rate constants for weathering of organic carbon (kwpy) and CaSO₄ sulfur (kwpy) also showed negligible variation in O₂. (However, increasing the initial mass of young pyrite sulfur by a factor of ten led to too low O₂ values for the present.)

Variation of initial values from those shown in Table 1 for most of the remaining parameters show variations that can be plotted and these are illustrated in Figs. 6–11. Figs. 6 and 7 show that variations of 50–200%, from the standard values of Table 1, in the rate constants for young pyrite-S weathering (kwpy) and young carbonate-C weathering (kwpy) result in distinct differences in the late

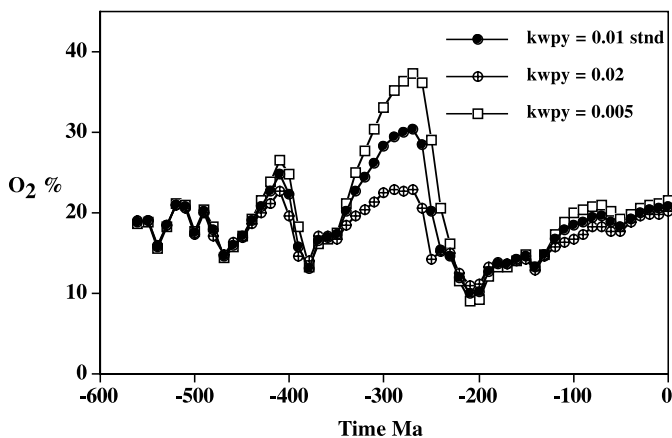


Fig. 6. Plot of O₂ vs time showing the effects of varying the rate constant for the weathering of young pyrite (kwpy). stnd = standard value (Table 1).

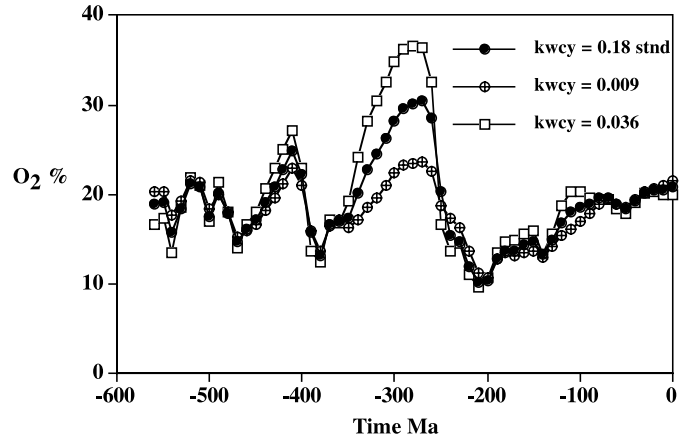


Fig. 7. Plot of O₂ vs time showing the effects of varying the rate constant for the weathering of young carbonates (kwpy).

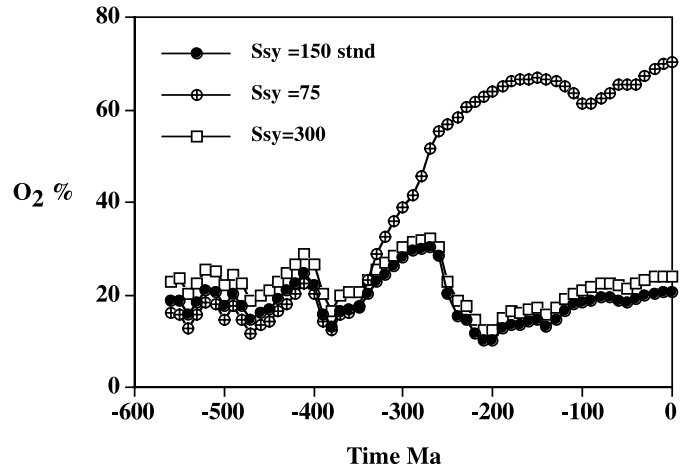


Fig. 8. Plot of O₂ vs time showing the effects of varying the initial starting mass of young CaSO₄ sulfur (Ssy). Values are in 10¹⁸ moles.

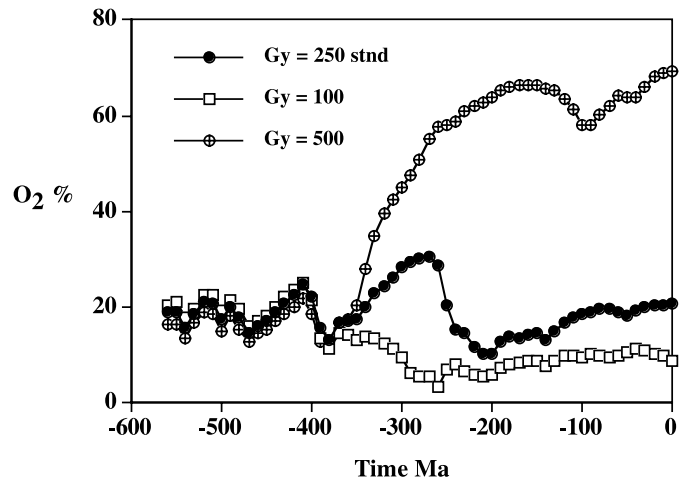


Fig. 9. Plot of O₂ vs time showing the effects of varying the initial mass of young organic carbon (Gy). Values are in 10¹⁸ moles.

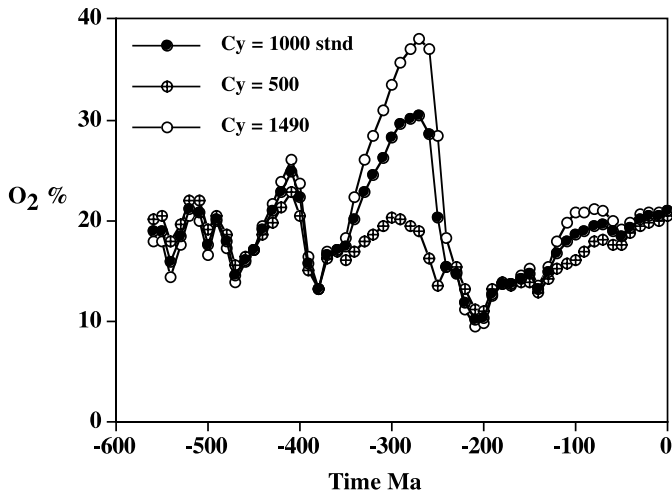


Fig. 10. Plot of O_2 vs time showing the effects of varying the initial mass of young carbonate carbon. Values in 10^{18} moles.

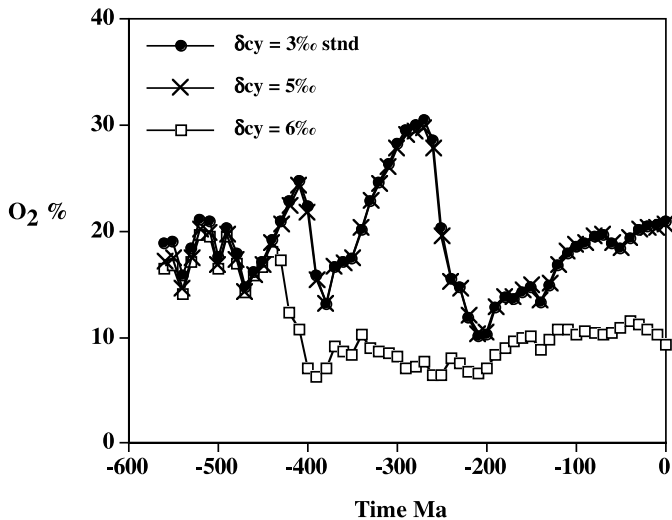


Fig. 11. Plot of O_2 vs time showing the effects of varying the initial $\delta^{13}C$ of young carbonate (δcy).

Paleozoic maximum for O_2 , but with the attainment of approximately correct values for present O_2 .

Other parameters show greater sensitivity towards O_2 . Variation of the mass of initial $CaSO_4$ sulfur between 50 and 200% (Fig. 8) results in values similar to the standard O_2 curve for a doubling but unreasonable values for a halving. The plot for varying initial masses of young organic carbon (Gy) between 40% and 200% (Fig. 9) results in unreasonable values for O_2 over time which do not attain the present value. Extreme high sensitivity is shown for the initial value of the mass of young carbonate carbon (Cy). Fig. 10 shows the effect of varying Cy from 50% to 149% but if the mass is raised from 149.0% to 149.1%, the mass of young organic carbon (Cy) and its rate of weathering become negative and O_2 will not plot. Another highly sensitive effect is shown by the initial value of $\delta^{13}C$ for young carbonate carbon. If $\delta^{13}C$ is allowed to rise from the standard value of 3‰ to 5‰, there is a negligible effect,

but when further raised to 6‰, unreasonably low values of O_2 result (Fig. 11). If $\delta^{13}C$ rises further to 7‰, O_2 goes negative. These calculations illustrate that the effects of the choice of initial conditions can vary, and that values of some parameters are constrained much more than are others. Because of the greater effect of the carbon cycle on O_2 than the sulfur cycle, the initial values chosen for some carbon parameters can become critical. This is especially true of the young initial masses of organic C and carbonate C and their isotopic composition, as demonstrated above.

2.4. Carbon isotope fractionation and O_2

The standard (GEOCARB) situation applied to GEOCARBSULF is based on the compilation of data by Hayes et al. (1999) for the difference in $\delta^{13}C$ between carbonate carbon and organic carbon, denoted as α_c . Another approach is the combination of α_c values from Hayes et al. for 550–200 Ma with those compiled recently by Katz et al. (2005) for the past 200 million years which are on the average about 2‰ smaller than those of Hayes et al. for this period. This suggests a simplified third approach which is to constantly subtract 2‰ from the Hayes et al. values for all times. A fourth approach is to use the dependence of α_c on the level of atmospheric O_2 (Berner, 2001) here using the equation:

$$\alpha_c(\text{‰}) = 30 + 4(O_2/38 - 1) \quad (4)$$

where O_2 = mass of O_2 in the atmosphere at time t and 38 is the mass at present (in 10^{18} moles). Results of the four approaches are shown in Fig. 12. The differences between the Hayes et al. and Katz et al. data cannot be ascribed to different mixtures of terrestrially derived organic matter of lower $\delta^{13}C$ because in both studies it is stated that the carbon isotopic data are believed to be based solely on marine organic matter. At any rate it is possible that both

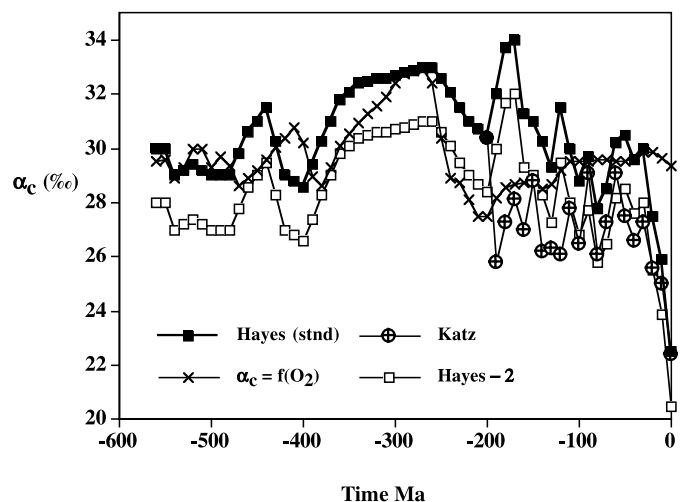


Fig. 12. Difference of $\delta^{13}C$ for carbonate carbon– $\delta^{13}C$ for organic carbon, α_c , as a function of time. References are Hayes et al. (1999); Katz et al. (2005). $\alpha_c = f(O_2)$ is for the expression: $\alpha_c = 30 + 4(O_2/38 - 1)$ (Berner, 2001). Hayes - 2 is Hayes et al. values–2‰.

sets of data may be in error because much terrestrially derived organic matter is buried both on land (Stallard, 1998) and in the sea and it is generally of a different isotopic composition than marine organic matter.

Comparison of the effect on atmospheric O₂ of using the four different isotopic fractionation values α_c is shown in Fig. 13. From the viewpoint of the entire Phanerozoic, the different α_c data sets result in no large differences in derived O₂ curves even though the values for α_c differ appreciably at various times. This means that the overall shape of the standard O₂ curve is not highly dependent on the exact values chosen for carbon isotopic fractionation.

Besides differences in α_c , there are also differences in the values reported for $\delta^{13}\text{C}$ of carbonates (representing the ocean) between the data of Lindh (1983) and Katz et al. (2005) for the past 200 million years (see Fig. 1). As an additional sensitivity check Fig. 14 is presented to illustrate the effect on O₂ over the past 200 million years of the differences in both α_c (Hayes vs Katz) and carbonate $\delta^{13}\text{C}$ (Lindh vs Katz). There is no major change in the general trend of O₂ vs time for Jurassic to recent for the two data sets (Hayes + Lindh; Katz). However, with the Katz data set there are two prominent maxima in O₂ centered at 150 Ma (Jurassic) and 20 Ma (Neogene). It remains to be seen whether these maxima are real; there is no independent evidence for them. Until the Jurassic and Neogene O₂ maxima are proved to be correct, the earlier data sets of Lindh for Jurassic to recent carbonate $\delta^{13}\text{C}$ and Hayes et al. for Phanerozoic α_c are used as a provisional standard formulation. In this way, at least all values of α_c are from the same Hayes et al. (1999) data set.

2.5. Sulfur isotope fractionation and O₂

In the paper by Berner (2001), it was shown that the fractionation of sulfur isotopes, expressed as the difference

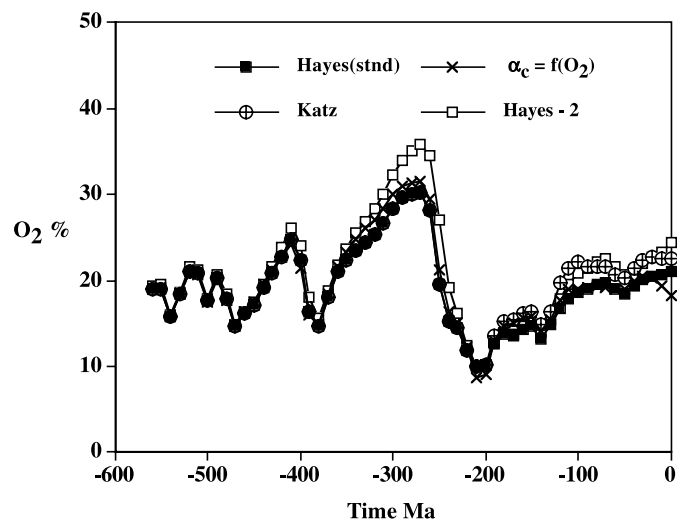


Fig. 13. Plot of O₂ vs time based on different α_c values (see caption for Fig. 12 for references).

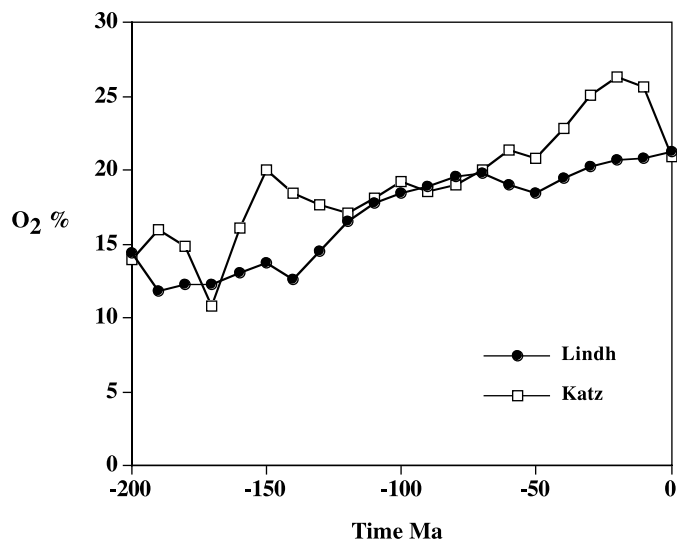


Fig. 14. Plot of O₂ vs time for the past 200 million years based on the $\delta^{13}\text{C}$ data of Lindh (1983) (combined with the α_c data of Hayes et al., 1999) compared to O₂ derived from the $\delta^{13}\text{C}$ and α_c data of Katz et al. (2005).

between $\delta^{34}\text{S}$ for CaSO₄ sulfur and pyrite sulfur, can be expressed by the equation:

$$\alpha_s(\text{‰}) = 35(\text{O}_2/38)^n \quad (5)$$

where α_s is the fractionation in ‰, O₂ is the mass of O₂ in the atmosphere (in 10¹⁸ moles), 38 is the present day mass, and n is an empirical parameter. This expression, that provides additional negative feedback against excessive O₂ variation, is used for the standard formulation of the present paper. (Negative feedback is provided by using the oxygen level calculated at step t to compute α_s and then O₂ at step $t + 1$. Although not strictly numerically correct, this procedure does not lead to appreciable changes in overall trends in O₂ vs time as shown by reverse modeling (K. Fennel and S. Petsch, personal communication). Eq. (5) is based on the assumption that higher atmospheric O₂ leads to greater re-oxidation and cycling of sulfur by bioturbation at the sediment water interface leading to greater sulfur isotope fractionation (Canfield and Teske, 1996). Sensitivity of α_s to the variation of n from 0.5 to 2.0 is shown in Fig. 15. (Letting $n = 0$, in other words having a constant sulfur isotope fractionation over time, results in physically impossible negative O₂ masses for the early Paleozoic—see Berner, 2001). Fig. 15 shows that appreciable variation of α_s with changing n occurs only during the late Paleozoic when O₂ values were very high. The standard value adopted for n was 1.5 which gives a range in α_s of from 10‰ to 70‰. This is in keeping with the range of variation for measured natural samples also shown in Fig. 15 (Strauss, 1999).

The effect on O₂ of varying α_s , as n varies, is shown in Fig. 16. Large differences are shown for the past 220 million years (Triassic to recent) with higher values of n resulting in less variation of O₂ over time due to increased negative feedback (Berner, 2001). The standard value of $n = 1.5$ was adopted as a compromise to prevent the

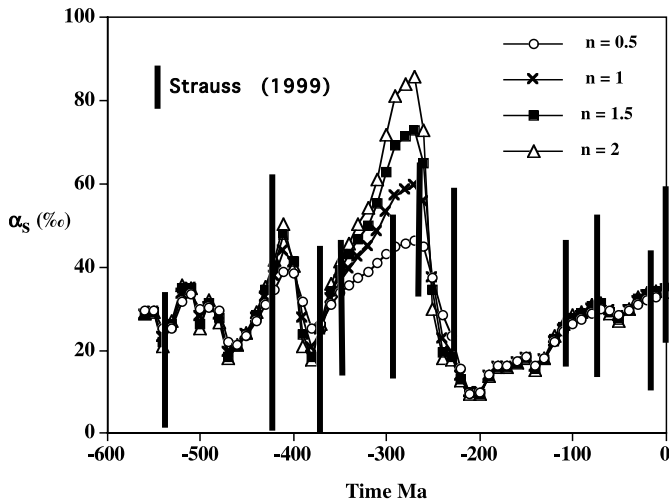


Fig. 15. Difference of $\delta^{34}\text{S}$ for CaSO_4 sulfur– $\delta^{34}\text{S}$ for pyrite sulfur, α_s , as a function of time for variable n . $\alpha_s(\text{‰}) = 35 (\text{O}_2/38)^n$. Range of measurements of Strauss (1999) are shown for comparison.

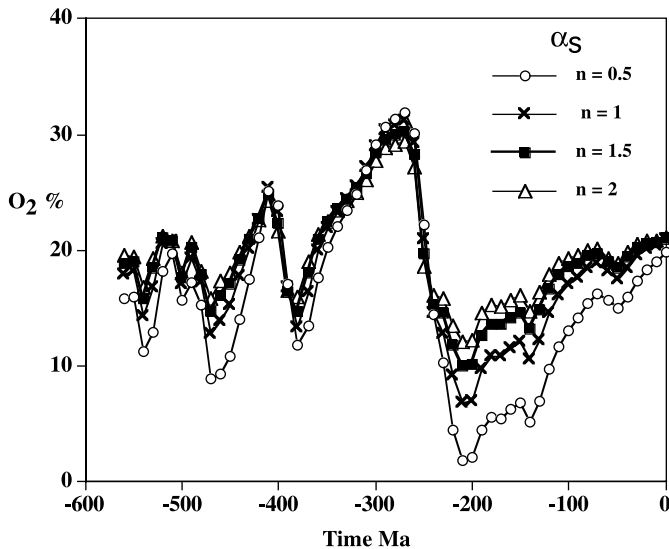


Fig. 16. Plot of O_2 vs time for different α_s based on varying values of n (see caption to Fig. 15).

attainment of excessively low O_2 values during the Triassic while keeping the range of α_s (10–70‰) within the limits measured on rocks (Strauss, 1999). Concentrations of O_2 less than about 12% are inimical to the formation of forest fires which must have existed throughout post-Devonian time because of the presence of fossil charcoal (Chaloner, 1989; Wildman et al., 2004b). By contrast with the Triassic to recent, values of O_2 during the late Paleozoic O_2 maximum (centered on 300 Ma) are rather insensitive to changes in α_s and n even though this is the time when values of α_s vary the most (Fig. 15). This results from the fact that the O_2 maximum is due mainly to increased rates of burial of organic carbon (high values of $\delta^{13}\text{C}$) and is negligibly affected by low rates of burial of pyrite sulfur (low values of $\delta^{34}\text{S}$) at the same time (Berner and Raiswell, 1983).

2.6. Land area, relief, erosion and O_2

In previous carbon and sulfur isotope mass balance models (e.g., Garrels and Lerman, 1984; Berner, 2001) rates of organic matter, pyrite, carbonate, and sulfate weathering were assumed to be affected only by changes in the mass of material undergoing weathering. This does not take into account other factors affecting weathering, such as increased exposure of rocks to the atmosphere by erosive stripping due to high relief, changes in land area exposed to weathering and changes in the degree of flushing of soils as represented by river runoff. These factors have all been applied to silicate and carbonate weathering in GEOCARB modeling. In GEOCARB-SULF non-dimensional weathering parameters $f(t)$ are applied to the weathering of organic matter, pyrite and CaSO_4 which are also applied to the weathering of silicates and carbonates as in GEOCARB modeling. (For a detailed discussion of non-dimensional weathering parameters see Berner, 2004). Weathering expressions for organic matter, pyrite and CaSO_4 introduced here are (weathering expressions for carbonates are the same as used in GEOCARB):

$$\text{Fwgy} = f_R(t)f_A(t)kwgy \text{ Gy} \quad (6)$$

$$\text{Fwga} = f_R(t)\text{Fwga}(0) \quad (7)$$

$$\text{Fwpy} = f_R(t)f_A(t)kwpy \text{ Spy} \quad (8)$$

$$\text{Fwpa} = f_R(t)\text{Fwpa}(0) \quad (9)$$

$$\text{Fwsy} = f_A(t)f_D(t)kwsy \text{ Ssy} \quad (10)$$

$$\text{Fwsa} = f_A(t)f_D(t)\text{Fwsa}(0) \quad (11)$$

where Fwgy, Fwpy, Fwsy = weathering rates of young organic-C, pyrite-S, and sulfate-S

Fwga, Fwpa, Fwsa = weathering rates of old organic carbon, pyrite-S, and sulfate-S with (0) referring to rates at present

Gy, Spy, Ssy = masses of young organic-C, pyrite-S, and sulfate-S

kwgy, kwpy, kwsy = rate constants for weathering

$f_R(t)$ = uplift factor reflecting the role of erosive stripping in chemical weathering

$f_A(t)$ = land area (t)/land area (0)

$f_D(t)$ = river runoff (t)/river runoff (0)

The inclusion of $f_R(t)$ in the weathering of both young and old organic matter and pyrite reflects the importance of erosive stripping in this process. Recent measurements and modeling of organic matter and pyrite weathering (Wildman et al., 2004a; Bolton et al., in press) indicate that erosive stripping is more important than changes in atmospheric O_2 level. Thus, no term for the dependence of weathering on O_2 level as a negative feedback (e.g., Bergman et al., 2004; Lasaga and Ohmoto, 2002) is employed. Additional dependence of the weathering of young organic matter and pyrite on land area $f_A(t)$ reflects the situation where sea level drop exposes freshly deposited sediments

to weathering. Erosive stripping is not thought to be important to the weathering of $CaSO_4$ because of its ability to dissolve in the subsurface; thus, $f_R(t)$ is not applied in this case. Instead $f_D(t)$ is used to reflect the dependence of $CaSO_4$ dissolution to water throughput or flushing and $f_A(t)$ is used to reflect the change of ground water level of coastal plains with changing sea level and land area.

The effect of changes in O_2 uptake via weathering of young and old organic matter pyrite, and $CaSO_4$ as affected by erosion rate $f_R(t)$, land area $f_A(t)$ and river runoff $f_D(t)$ (for sulfates) is shown in Fig. 17. When values of $f_R(t)$, $f_A(t)$ and $f_D(t)$ for organic matter, pyrite and sulfates are held at the present value of one for the entire Phanerozoic (as was done in the simpler model of Berner, 2001), there is notable change only during the late Paleozoic. This is in marked contrast to the important role of $f_R(t)$ in silicate weathering during the Mesozoic and Cenozoic (Berner, 2004). Apparently, the dominant influence on O_2 variability over most the Phanerozoic are changes in the burial rates of organic matter and pyrite and not in their weathering rates. Other weathering parameters affecting silicate weathering such as $f_E(t)$, reflecting the evolution of land plants, and $f_B(t)$, feedback due to changes in global temperature, were not applied to the weathering of organic matter, pyrite and $CaSO_4$ because root processes would have minimal effects on their weathering rate and the effects of temperature changes are small compared to the other effects considered here. The dissolution rate of highly soluble $CaSO_4$ minerals is affected far more by water availability than by temperature. Also, an additional run with changing temperature applied to the weathering of young organic matter and pyrite made little difference in results for O_2 vs time.

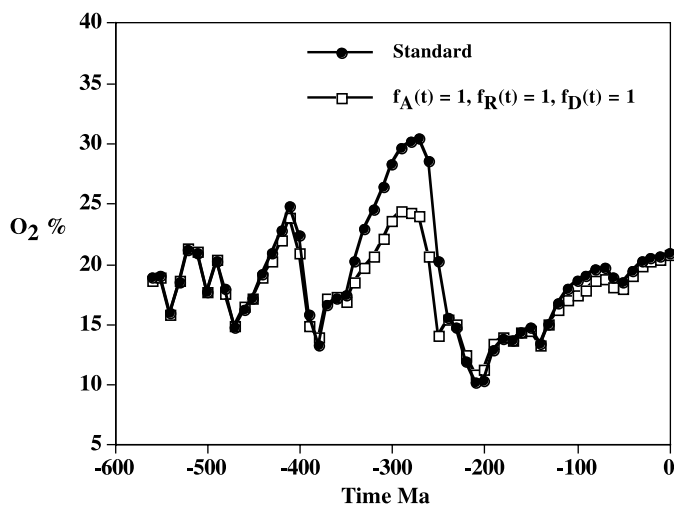


Fig. 17. Plot of O_2 vs time for the standard situation vs that for constant tectonic uplift and erosional stripping ($f_R(t) = 1$), constant land area ($f_A(t) = 1$) and constant river runoff ($f_D(t) = 1$) as they affect the weathering of organic matter, pyrite and $CaSO_4$ over time.

2.7. Atmospheric carbon dioxide

Introduction of new carbon isotopic data and rapid recycling to GEOCARB modeling for CO_2 , as is done in the present paper, should result in differences in calculated past levels of CO_2 from that obtained by GEOCARB modeling alone. The effect is due to change in rates of weathering and burial of organic matter and carbonates and to the confinement of metamorphic/volcanic/diagenetic degassing to “old” carbonate and organic matter only. Rapid recycling and separation of rocks into “young” and “old” is not applied to silicate weathering because no simple negative feedback would result. Silicate weathering in GEOCARB is confined mainly to highly weatherable primary calcium and magnesium silicates (e.g., plagioclase, biotite, pyroxenes) and such minerals do not form in sediments. Thus, there is no simple recycling, via “rapid” burial, uplift and weathering, as there is for organic matter, pyrite, carbonates and calcium sulfates.

For sensitivity purposes, the effects of discriminating the weathering of volcanic rocks from that for non-volcanic silicates is considered, based on the recent work of Berner (in press). The changing proportion over time of volcanic weathering, which is faster than non-volcanic weathering (Meybeck, 1987), is derived from the strontium isotopic composition of Phanerozoic seawater, and assumed fixed values of $^{87}Sr/^{86}Sr$ for volcanic and non-volcanic silicates.

Comparison of results for RCO_2 vs time, where RCO_2 is the ratio of the mass of atmospheric CO_2 at some past time to that at “present” (pre-human mean for Pleistocene or past 1 million years), for GEOCARB vs GEOCARBSULF is shown in Fig. 18. Curves are shown for including and not including volcanic weathering so as to discriminate the effects on GEOCARBSULF of the effects of (organic) rapid recycling alone from those due to volcanic weathering plus rapid recycling (Berner, in press). From an overall Phanerozoic perspective there is little change in the overall trend of CO_2 vs time. This illustrates the dominance of silicate weathering and metamorphic/volcanic/diagenetic degassing over that of organic matter burial and weathering. There are some notable differences during the early-to-mid Paleozoic (550–350 Ma) and Mesozoic (250–100 Ma) but within the estimated range of modeling error (Berner and Kothavala, 2001; Berner, 2004; Royer et al., 2004). Most notably, for variable volcanic weathering, there is a deepening of the minimum during the Late Ordovician, and decreased RCO_2 values during the Mesozoic. The Late Ordovician low in CO_2 is in accord with a continental glaciation at that time.

All three curves of Fig. 18 agree in general with the range of independent CO_2 estimates and with the contention that CO_2 was a major driver of Phanerozoic climate (Royer et al., 2004). A notable feature of Fig. 18 is that the GEOCARBSULF (no volc) model results in a sharp peak in CO_2 at the Permian-Triassic boundary that is not duplicated at any other time during the Phanerozoic. This

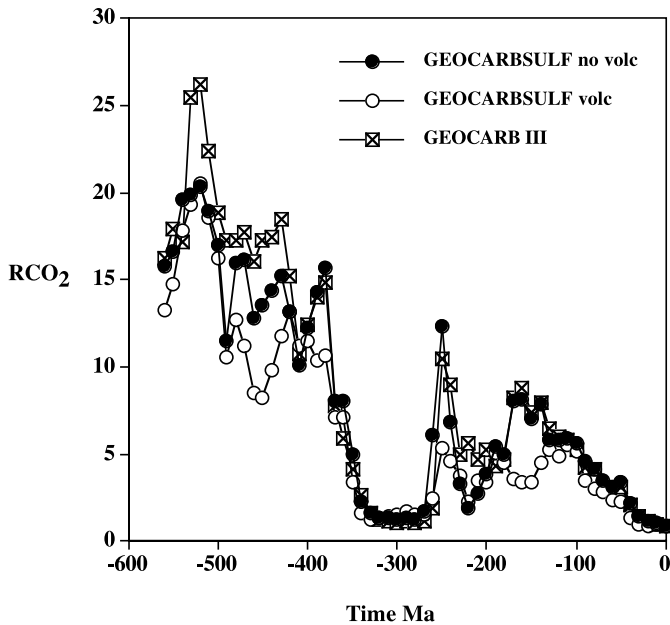


Fig. 18. Plots of RCO_2 vs time for GEOCARB (Berner and Kothavala, 2001) and GEOCARBSULF modeling. RCO_2 is the ratio of the mass of atmospheric CO_2 at a past time to that at present (weighted mean for the past million years). The terms (volc) and (no volc) refer to the addition or non-addition of variable volcanic weathering (Berner, in press) to the modeling.

is caused by a large drop in $\delta^{13}C$ across the boundary reflecting a reduction of CO_2 uptake by much lower organic matter burial accompanying the Permo-Triassic extinction (Berner, 2005; Grard et al., 2005) combined with increased input of volcanic CO_2 from Siberian volcanism (Grard et al., 2005). On a shorter, sub-million year time scale this peak is in fact sharper and higher. (GEOCARB and GEOCARBSULF models input smoothed data only every ten million years, thus missing short term events.)

3. Discussion and conclusions

The major observation of the results of GEOCARBSULF modeling is that there is little overall change in the curves of CO_2 and O_2 vs time from earlier GEOCARB and isotope mass balance modeling. To be sure there are some variations during the early Paleozoic for O_2 and CO_2 and during the Mesozoic for CO_2 due to the use of new carbon isotopic data (Fig. 1) and the introduction of variable volcanic rock weathering, but the general conclusions of the earlier studies are not changed. The most dominant factor affecting both CO_2 and O_2 over the past 550 million years was the rise of vascular land plants, namely trees (Berner, 2004). They brought about large increases in the rates of chemical weathering of silicates and rates of burial of organic matter resulting in a dramatic rise of O_2 and drop in CO_2 during the mid-to-late Paleozoic. These trends ended abruptly at the Permian-Triassic boundary as a result (and probably contributing cause) of the massive biological extinction at that time. The slow

general rise in O_2 since that time may have been due mainly to increased burial of organic matter on passive continental margin shelves (Falkowski et al., 2005).

If terrestrially derived material continued during the Mesozoic and Cenozoic to be an important component to global organic matter burial, then proper modeling must take this into account. Unfortunately, the available compilations of isotopic data for organic carbon for the past 200 million years (Lindh, 1983; Hayes et al., 1999; Katz et al., 2005) are all based only on marine sediments which likely contain mostly marine-derived organic matter. Much plant-derived organic carbon is buried on land in swamps, lakes etc. (Stallard, 1998) and in marginal marine environments such as deltas (Berner, 2004) and the isotopic composition of the terrestrial material normally differs from that of marine-derived organic matter. More data from such environments are needed for past times to obtain a better idea of the isotopic composition of all organic matter being buried globally.

The results of the present paper for O_2 can be compared to the model results of Bergman et al. (2004) whose curve of O_2 vs time is shown in Fig. 19. Both the Bergman and GEOCARBSULF results show a late Paleozoic maximum but results for the Mesozoic and Cenozoic (past 250 million years) differ considerably between the two studies. The Bergman approach is quite different from that of GEOCARBSULF in that isotopic data are not used to drive the modeling and, instead, various seemingly reasonable a priori assumptions are made concerning weathering, organic matter deposition, and negative feedbacks providing stabilization. The writer does not agree with two of their major assumptions. First of all, Bergman et al. assume that the weathering rate of organic matter and pyrite are proportional to the level of atmospheric oxygen (square root dependency of Lasaga and Ohmoto, 2002). This provides negative feedback. However, the field and modeling studies of Wildman et al. (2004a) and Bolton et al. (in press) show that, for a range of erosion rates around the

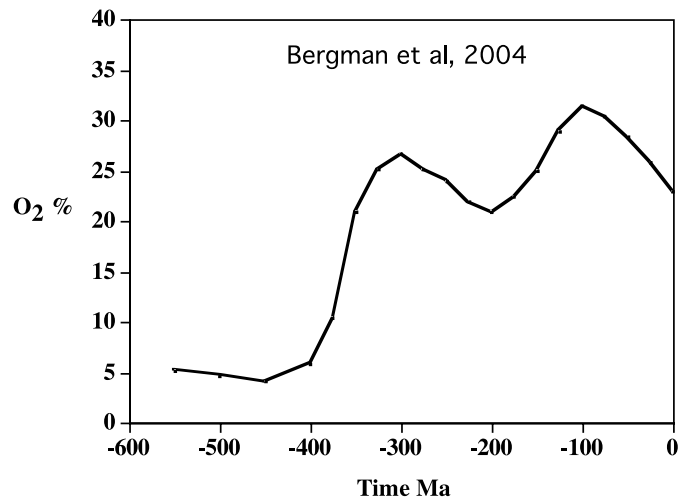


Fig. 19. Plot of O_2 vs time from Bergman et al. (2004).

present global mean, organic matter and pyrite weathering are limited by the rate of erosive stripping of overburden and exposure to the atmosphere and not by the availability of O₂. Second, Bergman et al. assume that marine organic matter burial is limited by the input to the oceans of phosphate from weathering on land. While production of organic matter undoubtedly is nutrient limited, burial also involves preservation. Berner and Canfield (1989) have shown that sediment deposition rate is a major control on the rate of burial and preservation of organic matter and pyrite in marine sediments. Most organic burial occurs at present in deltaic and shelf regions where high burial rates are due to very high sedimentation rates even though organic carbon and pyrite concentrations are relatively low (Berner, 2004). Thus, changes in global rates of erosion, as reflected by changes in global rates of sedimentation, have a major effect on O₂ production during organic and pyrite burial. This factor is not considered by Bergman et al. (2004). During the Mesozoic and Cenozoic there were great changes in erosion and sedimentation rates (Berner, 2004, in press) and failure to consider this may help explain some of the differences between the Bergman study and GEOCARBSULF for this time span.

The “best estimate” or standard curve for O₂ along with a crude estimate of the range of error based partly on the sensitivity analyses of the present paper is shown in Fig. 20. The best estimate uses the data of Korte et al. (2005b) for Triassic $\delta^{13}\text{C}$ because it allows for no O₂ concentrations to fall below 12%. (In the sensitivity studies shown earlier the Lindh Triassic data were used which made little difference as far as overall results are concerned). Forest fires appear to be limited by O₂ levels below

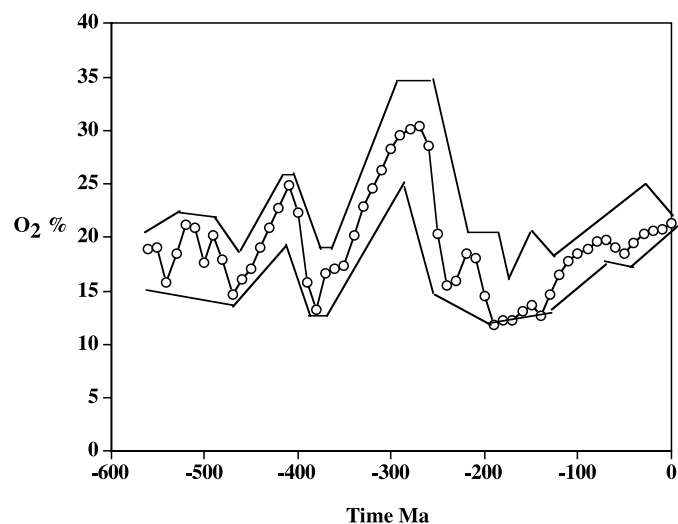


Fig. 20. Plot of O₂ vs time for the standard GEOCARBSULF model with a crude estimate of the range of error based on sensitivity study. Triassic O₂ values differ from those shown in the other plots of the present study because of the use of alternative $\delta^{13}\text{C}$ data (Korte et al., 2005a,b; see Fig. 1). This enables O₂ concentrations to be equal to or in excess of 12%, the value believed to be the minimum to support forest fires (Chaloner, 1989; Wildman et al., 2004b).

12% (Chaloner, 1989; Wildman et al., 2004b) and there is evidence for fires in the form of charcoal at this time (Scott, 2000). Range of error also includes the effects of using the alternate carbon isotopic data of Korte et al. (2005a) for the Permian and Katz et al. (2005) for the Jurassic to recent (see Fig. 1).

The O₂ curve may have an important, relatively unrecognized relation to animal evolution. It is believed to have been a contributing factor to animal gigantism during the Permo-Triassic (Graham et al., 1995), to extinction at the Permo-Triassic boundary (Huey and Ward, 2005), to mammalian evolution (Falkowski et al., 2005) and to Phanerozoic animal evolution in general (Ward, in press). Based on this initial work, the writer looks forward to more research on the subject of changing O₂ level and paleophysiology.

Acknowledgements

Research was supported by Grant DE-FG02-01ER15173 of the U.S. Department of Energy. The writer acknowledges helpful discussions with Peter Ward, Ray Huey, Mimi Katz, and Katja Fennel and helpful reviews by Yves Godderis and Fred Mackenzie.

Associate editor: Donald E. Canfield

References

- Arvidson, R.S., Mackenzie, F.T., 2006. MAGic: A phanerozoic model for the geochemical cycling of major-rock-forming components. *Am. J. Sci.* **306**, 155–190.
- Bergman, N.M., Lenton, T.M., Watson, A.J., 2004. COPSE: a new model of biogeochemical cycling over Phanerozoic time. *Am. J. Sci.* **304**, 397–437.
- Berner, R.A., 1987. Models for carbon and sulfur cycles and atmospheric oxygen: application to Paleozoic history. *Am. J. Sci.* **287**, 177–196.
- Berner, R.A., 2001. Modeling atmospheric O₂ over Phanerozoic time. *Geochim. Cosmochim. Acta* **65**, 685–694.
- Berner, R.A., 2004. *The Phanerozoic Carbon Cycle: CO₂ and O₂*. Oxford University Press, Oxford, 150p.
- Berner, R.A., 2005. The carbon and sulfur cycles and atmospheric oxygen from Middle Permian to Middle Triassic. *Geochim. Cosmochim. Acta* **69**, 3211–3217.
- Berner, R.A., 2006. Inclusion of the weathering of volcanic rocks in the GEOCARBSULF model. *Am. J. Sci.* **306** (in press).
- Berner, R.A., Canfield, D.E., 1989. A new model of atmospheric oxygen over Phanerozoic time. *Am. J. Sci.* **289**, 333–361.
- Berner, R.A., Kothavala, Z., 2001. GEOCARB III: a revised model of atmospheric CO₂ over Phanerozoic time. *Am. J. Sci.* **301**, 182–204.
- Berner, R.A., Raiswell, R., 1983. Burial of organic carbon and pyrite sulfur in sediments over Phanerozoic time: a new theory. *Geochim. Cosmochim. Acta* **47**, 855–862.
- Bolton, E.W., Berner, R.A., Petsch, S.T., 2006. The weathering of sedimentary organic matter as a control on atmospheric O₂: II. Theoretical modeling. *Am. J. Sci.* **306** (in press).
- Canfield, D.E., Teske, A., 1996. Late Proterozoic rise in atmospheric oxygen concentration inferred from phylogenetic and sulphur-isotope studies. *Nature* **382**, 127–132.
- Chaloner, W.G., 1989. Fossil charcoal as an indicator of paleoatmospheric oxygen level. *J. Geol. Soc. London* **14**, 171–174.
- Ebelmen, J.J., 1845. Sur les produits de la decomposition des especes minérales de la famille des silicates. *Ann. Rev. des Moines* **12**, 627–654.

- Falkowski, P., Katz, M., Milligan, A., Fennel, K., Cramer, B., Aubry, M.P., Berner, R.A., Zapol, W.M., 2005. The rise of atmospheric oxygen levels over the past 205 million years and the evolution of large placental mammals. *Science* **309**, 2202–2204.
- Francois, L.M., Walker, J.C.G., 1992. Modeling the Phanerozoic carbon-cycle and climate-constraints from the Sr-87/Sr-86 isotopic ratio of seawater. *Am. J. Sci.* **292**, 81–135.
- Garrels, R.M., Lerman, A., 1984. Coupling of the sedimentary sulfur and carbon cycles—an improved model. *Am. J. Sci.* **284**, 989–1007.
- Garrels, R.M., Mackenzie, F.T., 1971. *Evolution of Sedimentary Rocks*. W.W. Norton and Company, New York, 397 pp.
- Garrels, R.M., Perry, E.A., 1974. Cycling of carbon, sulfur and oxygen through geologic time. In: Goldberg, E. (Ed.), *The Sea*, v.5. Wiley, New York, pp. 303–316.
- Grard, A., Francois, L.M., Dessert, C., Dupre, B., Godderis, Y., 2005. Basaltic volcanism and mass extinction at the Permo-Triassic boundary: Environmental impact and modeling of the global carbon cycle. *Earth Planet. Sci. Lett.* **234**, 207–221.
- Godderis, Y., Francois, L.M., Veizer, J., 2001. The early Paleozoic carbon cycle. *Earth Planet. Sci. Lett.* **190**, 181–196.
- Graham, J.B., Dudley, R., Aguilar, N., Gans, C., 1995. Implications of the late Palaeozoic oxygen pulse for physiology and evolution. *Nature* **375**, 117–120.
- Hansen, K.W., Wallmann, K., 2003. Cretaceous and Cenozoic evolution of seawater composition, atmospheric O₂ and CO₂: a model perspective. *Am. J. Sci.* **303**, 94–148.
- Hayes, J.M., Strauss, H., Kaufman, A.J., 1999. The abundance of ¹³C in marine organic matter and isotope fractionation in the global biogeochemical cycle of carbon during the past 800 Ma. *Chem. Geol.* **161**, 103–125.
- Holland, H.D., 1978. *The Chemistry of the Atmosphere and Oceans*. Wiley, New York, 351p.
- Huey, R.B., Ward, P.D., 2005. Hypoxia, global warming, and terrestrial late Permian extinctions. *Science* **308**, 398–401.
- Kampschulte, A., Strauss, H., 2004. The sulfur isotopic evolution of Phanerozoic seawater based on the analysis of structurally substituted sulfate in carbonates. *Chem. Geol.* **204**, 255–286.
- Katz, M.E., Wright, J.D., Miller, K.G., Cramer, B.S., Fennel, K., Falkowski, P.G., 2005. Biological overprint of the geological carbon cycle. *Mar. Geol.* **217**, 323–338.
- Kirschvink, J.L., Raub, T.D., 2003. A methane fuse for the Cambrian explosion: carbon cycles and true polar wander. *Compte Rendus Geoscience* **335**, 65–78.
- Korte, C., Jasper, T., Kozur, H.W., Veizer, J., 2005a. $\delta^{13}\text{C}$ and $\delta^{18}\text{O}$ values of Permian brachiopods: A record of seawater evolution and continental glaciation. *Palaeogeogr. Palaeoclimatol. Palaeoecol.* **224**, 333–351.
- Korte, C., Kozur, H.W., Veizer, J., 2005b. $\delta^{13}\text{C}$ and $\delta^{18}\text{O}$ values of Triassic brachiopods and carbonate rocks as proxies for coeval seawater and palaeotemperature. *Palaeogeogr. Palaeoclimatol. Palaeoecol.* **226**, 287–306.
- Lasaga, A.C., Ohmoto, H., 2002. The oxygen geochemical cycle: dynamics and stability. *Geochim. Cosmochim. Acta* **66**, 361–381.
- Lindh T.B., 1983. Temporal variations in ¹³C and ³⁴S and global sedimentation during the Phanerozoic. Thesis. Univ. Miami. 98 pp (unpublished).
- Meybeck, M., 1987. Global chemical weathering of surficial rocks estimated from river dissolved loads. *Am. J. Sci.* **287**, 401–428.
- Mii, H.S., Grossman, E.L., Yancey, T.E., 1997. Stable carbon and oxygen isotope shifts in Permian seas of West Spitsbergen—Global change or diagenetic artifact? *Geology* **25**, 227–230.
- Mii, H.S., Grossman, E.L., Yancey, T.E., Chuvashov, B., Egorov, A., 2001. Isotopic records of brachiopod shells from the Russian Platform - evidence for the onset of mid-Carboniferous glaciation. *Chem. Geol.* **175**, 133–147.
- Popp, B.N., Anderson, T.F., Sandberg, P.A., 1986. Brachiopods as indicator of original isotopic compositions in some Paleozoic limestones. *Geol. Soc. Am. Bull.* **97**, 1262–1269.
- Royer, D.L., Berner, R.A., Montanez, I.P., Tabor, N.J., Beerling, D.J., 2004. CO₂ as a principal driver of Phanerozoic climate. *GSA Today* **14**, 4–10.
- Scott, A.C., 2000. The pre-Quaternary history of fire. *Palaeogeogr. Palaeoclim. Palaeoecol.* **164**, 281–329.
- Saltzman, M.R., 2005. Phosphorus, nitrogen, and the redox evolution of the oceans. *Geology* **33**, 573–576.
- Stallard, R.F., 1998. Terrestrial sedimentation and the carbon cycle: coupling weathering and erosion to carbon burial. *Global Biogeochem. Cycle* **12**, 231–257.
- Strauss, H., 1999. Geological evolution from isotope proxy signals—sulfur. *Chem. Geol.* **161**, 89–101.
- Sundquist, E.T., 1991. Steady state and non-steady state carbonate-silicate controls on atmospheric CO₂. *Quaternary Sci. Rev.* **10**, 283–296.
- Urey, H.C., 1952. *The Planets: their Origin and Development*. Yale University Press, New Haven, 245p.
- Veizer, J., Ala, D., Azmy, K., Bruckschen, P., Buhl, D., Bruhn, F., Carden, G.A.F., Diener, A., Ebner, S., Godderis, Y., Jasper, T., Korte, C., Pawellek, F., Podlaha, O.G., Strauss, H., 1999. ⁸⁷Sr/⁸⁶Sr, $\delta^{13}\text{C}$ and $\delta^{18}\text{O}$ evolution of Phanerozoic seawater. *Chem. Geol.* **161**, 59–88.
- Ward P.D., 2006, *A New History of Life; Respiration and Animal Design*, Natl. Acad. Press., in press.
- Wilde, P., 1987. Model of progressive ventilation of the late Precambrian-early Paleozoic ocean. *Am. J. Sci.* **287**, 442–459.
- Wildman, R.A., Berner, R.A., Petsch, S.T., Bolton, E.W., Eckert, J.O., Mok, U., Evans, J.B., 2004a. The weathering of sedimentary organic matter as a control on atmospheric O₂ I. Analysis of a black shale. *Am. J. Sci.* **304**, 234–249.
- Wildman, R.A., Hickey, L.J., Dickinson, M.B., Berner, R.A., Robinson, J.M., Dietrich, M., Essenhigh, R.H., Wildman, C.B., 2004b. Burning of forest materials under late Paleozoic high atmospheric oxygen levels. *Geology* **32**, 457–460.